JOURNAL OF MAGNETIC RESONANCE **135,** 427–434 (1998)
ARTICLE NO. MN981562

Simulation of CPMAS Signals at High Spinning Speeds

Siddharth Ray, Vladimir Ladizhansky, and Shimon Vega

Department of Chemical Physics, Weizmann Institute of Science, 76100 Rehovot, Israel

Received January 9, 1998; revised July 14, 1998

The spin dynamics of an $S(\frac{1}{2})I_N$ system during the CP mixing time of continuous wave and variable amplitude cross-polarization magic angle spinning (CWCPMAS and VACPMAS) experiments is discussed. The signal enhancement of a low abundant S spin, coupled to a set of $N = 6$ coupled spins with $I = \frac{1}{2}$, is evaluated as a function of the length of the mixing time. For CWCPMAS this signal is first evaluated in the frequency domain and then transformed to the time domain. These calculations provide some additional insight into the CP spin dynamics and enable a practical approach toward the evaluation of CP signals of large spin systems. In addition the adiabatic character of the ramped VACPMAS experiments is discussed and S-spin signals of a spin system with $N = 6$ are simulated. Estimates of the upper bounds of the CP signals as a function of the number of I spins in an $S(\frac{1}{2})I_N$ system are given and compared with the calculated values.

INTRODUCTION

In a previous publication (*1*) we discussed some basic principles of cross-polarization (CP) experiments on nonrotating (*2*) and rotating samples (*3*). For magic angle spinning (MAS) we based our theoretical description on Floquet formalism (*4, 5*). A description of the spin dynamics during the CP process of an $S(\frac{1}{2})I_N$ spin system was presented, but no calculations of the S-spin signals using this formalism were reported. Here we present some simulated S-spin signals of CPMAS experiments on an $S(\frac{1}{2})I_6$ spin system. As was discussed in Ref. (*1*), the CP process can be described by the equilibration of spin populations between spin-energy level manifolds. For this publication we designed a computer program, based on this approach, that was used to evaluate the signals of CPMAS experiments on systems of up to seven spins. The analogy between the buildup of the CP signals and the free induction decay signals of a single heteronuclear spin, interacting with a set of coupled homonuclear spins, will allow us to use this program for the simulation of buildup curves of real experimental CP signals and their Fourier transforms.

In many laboratories it has become standard procedure to use ramped variable amplitude cross polarization (*6, 7*). By doing so an exact setting of the Hartmann–Hahn (H–H) (*8*) condition is not necessary and an extra enhancement of the CP signal is obtained due to the adiabatic character of these VACPMAS experiments (*9*). A large variety of amplitude- and phase-modulated rf fields were applied during the CP mixing time to improve signal enhancement and lower the effect of rf inhomogeneities (*7*). The adiabatic character of these techniques was discussed extensively and demonstrated experimentally (*6, 7*). The spin physics of CWCPMAS as well as of VACPMAS on small spin systems has been presented and it has been shown that Floquet theory provides a convenient theoretical framework for describing the experimental results (*7*). The CP spin dynamics has already been discussed more than 20 years ago and since then has been the subject of a variety of additional studies (*10–12*).

In this publication we use the Floquet spin state formalism to simulate the CPMAS signals (*1*). At first the Hamiltonian of an $S(\frac{1}{2})I_N$ spin system, consisting of one low abundant spin coupled via the heteronuclear dipolar interaction to a set of N homonuclear-coupled spins I, is defined and the CPMAS S-spin signal is obtained by calculating the CP frequency spectrum. Then some calculated S-spin CPMAS enhancement curves for $N = 6$ are shown and analyzed. This discussion is extended to a simple ramped amplitude CPMAS experiment, and again some simulated time-dependent S signals are shown. In both cases an upper bound for the CP signals as a function of the number of homonuclear spins, N, in the system is estimated and compared with the calculated values. At high spinning speeds the observed CP spin dynamics is almost independent of the homonuclear interaction. This is demonstrated for CWCPMAS signal enhancements.

THE CPMAS HAMILTONIAN

The spin Hamiltonian of an $S(\frac{1}{2})I_N$ system, irradiated by two rf fields at the Larmor frequencies of the I and the S spins, in the doubly rotating frame has the form (*2*)

$$H = -\omega_{1I}I_z - \omega_{1S}S_z - \frac{1}{2}\sum_{i<j} a_{ij}(t)(3I_{zi}I_{zj} - \mathbf{I}_i \cdot \mathbf{I}_j) + \sum_i b_i(t)I_{xi}S_x, \quad [1]$$

where the homonuclear interaction terms are truncated with respect to the rf irradiation term $\omega_{1I}I_z$. The z directions of the I and S spins are chosen parallel to the the rf field directions.

1090-7807/98 $25.00

The coefficients of the homonuclear and heteronuclear dipolar terms are time-dependent due to sample spinning and contain $\exp\{ik\omega_R t\}$ terms with $k = -2, -1, +1, +2$ (*13*). To simplify the discussion we ignored all chemical shift terms in the Hamiltonian of Eq. [1]. The matrix representation of this Hamiltonian in Floquet space, defined by the manifolds of dressed states $|M_p\alpha n\rangle$ and $|M_p\beta n\rangle$ with $p = 1, \ldots, n_M$, can be evaluated by calculating the rf elements,

$$\langle M_p\alpha n|H_F^{rf}|M_p\alpha n\rangle = n\omega_R + M\omega_{1I} + \tfrac{1}{2}\omega_{1S}$$
$$\langle M_p\beta n|H_F^{rf}|M_p\beta n\rangle = n\omega_R + M\omega_{1I} - \tfrac{1}{2}\omega_{1S}, \qquad [2]$$

the homonuclear dipolar interaction elements,

$$\langle M_p\alpha n|H_F^{II}|M_p\alpha n + k\rangle = \langle M_p\beta n|H_F^{II}|M_p\beta n + k\rangle = \sum_{i<j} \alpha^{ij}(M_{pp})a_k^{ij}$$
$$\langle M_p\alpha n|H_F^{II}|M_q\alpha n + k\rangle = \langle M_p\beta n|H_F^{II}|M_q\beta n + k\rangle = \sum_{i<j} \alpha^{ij}(M_{pq})a_k^{ij}, \qquad [3]$$

and the heteronuclear dipolar interaction elements,

$$\langle M_p\alpha n|H_F^{IS}|(M \pm 1)_q\beta n + k\rangle = \sum_{i=1}^{N} \alpha^i(M_{pq}^{\pm})b_k^i, \qquad [4]$$

with

$$a_k^{ij} = \frac{1}{4}\frac{\gamma_I^2\mu_0\hbar}{r_{ij}^3}\, G_{|k|}^{ij}\exp\{ik\phi_{ij}\}$$
$$b_k^i = \frac{1}{4}\frac{\gamma_I\gamma_S\mu_0\hbar}{r_{ij}^3}\, G_{|k|}^{i}\exp\{ik\phi_i\} \qquad [5]$$

and the coefficients

$$\alpha^{ij}(M_{pq}) = 2\langle M_p|(3I_{zi}I_{zj} - \mathbf{I}_i\cdot\mathbf{I}_j)|M_q\rangle$$
$$\alpha^{i}(M_{pq}^{\pm}) = 2\langle M_p|I_{xi}|(M \pm 1)_q\rangle. \qquad [6]$$

For each pair p, q there can be only one coefficient $\alpha^{ij} = -1$ and $\alpha^i = 1$. The number of I-spin states in the manifolds $\{|M\alpha n\rangle\}$ are n_M, $p, q = 1, \ldots, n_M$; α and β are the spin-up and spin-down states of the S spin and $n = -\infty, \ldots, \infty$ are the Fourier indices. The G^{ij} and G^i coefficients are geometric functions of the polar angles (θ_{ij}, ϕ_{ij}) and (θ_i, ϕ_i) of the homo- and heteronuclear dipolar vectors $\mathbf{r}_{ij}$ and $\mathbf{r}_i$ in the rotor frame, respectively (*14*).

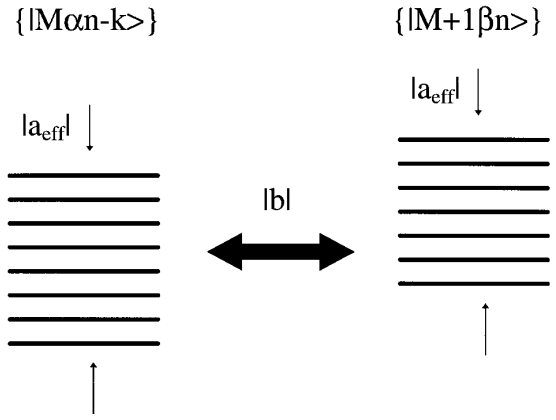

FIG. 1. A schematic representation of the interacting Floquet state manifolds $\{|M\alpha n - k\rangle\}$ and $\{|M + 1\beta n\rangle\}$ at the $\Delta n = k$ Hartmann–Hahn condition. The spread of the n_M and n_{M+1} energy levels, induced by the homonuclear dipole–dipole interaction, is reduced by the spinning speed and is schematically represented by the parameter $|a_{eff}|$. The effective heteronuclear interactions at the H–H condition are represented by $|b|$.

For rf fields that satisfy one of the Hartmann–Hahn conditions (*3*) $\omega_{1I} \approx \omega_{1S} + k\omega_R$, the Floquet matrix can be divided into block diagonals that are represented in the manifold of states $\{|M\alpha n\rangle, |(M + 1)\beta m\rangle\}$ (see Fig. 1) (*1*). The states in the two manifolds $\{|M\alpha n\rangle\}$ and $\{|M + 1\beta n + k\rangle\}$ are coupled via the heteronuclear interaction for all values $M < N/2$, whereas the states in $\{|(N/2)\alpha n\rangle\}$ and $\{|(-N/2)\beta n\rangle\}$ are not coupled to respective β and α states. For a number of N-coupled I spins the actual dimension of each diagonal block is $(n_M + n_{M+1})N_f$, where $N_f = 2n_f + 1$ is the number of dressed states defining the dimension of the truncated Hamiltonian, $n = -n_f, \ldots, n_f$. For example, for $N = 6$ and with $N_f = 11$ these dimensions are equal to 77, 231, 385, 385, 231, and 77 for $M = 2, 1, 0, -1, -2$, and -3 and $n_M = 6, 15, 20, 15, 6$, and 1, respectively, whereas $\{|3\alpha n\rangle\}$ and $\{|-3\beta n\rangle\}$ are not interacting with other manifolds.

To simulate the S-spin signal after a CPMAS mixing period the block diagonals must be constructed and diagonalized. The resulting eigenvalues $\lambda_n^r(M)$ and eigenvectors $|\lambda_n^r(M)\rangle$, with $r = 1, \ldots, (n_M + n_{M+1})$, govern the time-dependent CP S signals. Numerical diagonalization of the matrices becomes impractical for large N and N_f values. Here we have restricted ourselves to $N \le 6$ and $N_f = 13$.

CWCPMAS SIGNALS

In a conventional constant amplitude CPMAS experiment the initial state of the I spins is prepared by a $\pi/2$ pulse. Thus at the start of the CP mixing time, $t = 0$, the normalized Floquet density matrix, $R(0)$, has nonzero ma-

trix elements (*5*) (corresponding to the initial spin density matrix I_z)

$$\langle M_p\alpha n|R(0)|M_p\alpha n\rangle = \langle M_p\beta n|R(0)|M_p\beta n\rangle = Z^{-1}\beta_L M\omega_{0I} \quad [7]$$

with ω_{0I} the *I*-spin Larmor frequency. The intensity of the *S* signal at the end of the mixing period *t* is proportional to the time-dependent expectation value of S_z. The Floquet operator, Z_S, which corresponds to S_z, has matrix elements (*5*) given by

$$\langle M_p\alpha n|Z_S|M_p\alpha n\rangle = -\langle M_p\beta n|Z_S|M_p\beta n\rangle = 1/2, \quad [8]$$

and the normalized *S* signal can be written as

$$S(t) = S_0^{-1}\{S(N/2) + \sum_{M=-N/2}^{N/2-1}\sum_{n=-\infty}^{\infty} S_n^M(t)\exp\{in\omega_R t\}\}. \quad [9]$$

The normalization factor S_0^{-1} is equal to the inverse of the *S* signal after a single $\pi/2$ pulse (*5*)

$$\begin{aligned} S_0 &= Z^{-1}\beta_L\omega_{0S}\sum_{M=-N/2}^{N/2}\{\sum_{p=1}^{n_M}\langle M_p\alpha 0|Z_S^2|M_p\alpha 0\rangle \\ &\quad + \sum_{q=1}^{n_M}\langle M_q\beta 0|Z_S^2|M_q\beta 0\rangle\} \\ &= \frac{1}{2}Z^{-1}\beta_L\omega_{0S}\{\sum_M n_M\} \end{aligned} \quad [10]$$

with ω_{0S} the *S*-spin Larmor frequency. The first term in the curly braces in Eq. [9] is the signal resulting from the noninteracting manifolds $\{|N/2\alpha n\rangle\}$ and $\{|-N/2\beta n\rangle\}$. The density matrix elements $\langle N/2\alpha n|R(t)|N/2\alpha n\rangle = Z^{-1}\beta_L\omega_{0I}N/2$ and $\langle -N/2\beta n|R(t)|-N/2\beta n\rangle = -Z^{-1}\beta_L N/2$ are time-independent, and

$$\begin{aligned} S(N/2) &= \langle N/2\alpha 0|R(t)\,Z_S|N/2\alpha 0\rangle \\ &\quad + \langle -N/2\beta 0|R(t)\,Z_S| - N/2\beta 0\rangle \\ &= Z^{-1}\beta_L\omega_{0I}\{N/2\}, \end{aligned} \quad [11]$$

The time-dependent coefficients $S_n^M(t)$ are contributions from the manifolds $\{|M\alpha n\rangle, |M+1\beta m\rangle\}$

$$\begin{aligned} S_n^M(t) &= \sum_{p=1}^{n_M}\langle M_p\alpha n|R(t)\,Z_S|M_p\alpha 0\rangle \\ &\quad + \sum_{q=1}^{n_{M+1}}\langle (M+1)_q\beta n|R(t)\,Z_S|(M+1)_q\beta 0\rangle \\ &= \frac{1}{2}\sum_{p=1}^{n_M}\langle M_p\alpha n|R(t)|M_p\alpha 0\rangle \\ &\quad - \frac{1}{2}\sum_{q=1}^{n_{M+1}}\langle (M+1)_q\beta n|R(t)|(M+1)_q\beta 0\rangle. \end{aligned} \quad [12]$$

The matrix elements in these expansions are time-dependent and oscillate with frequencies that are equal to the Floquet energy differences.

At $t = 0$ only the elements with $n = 0$ are different from zero

$$S_0^M(0) = Z^{-1}\beta_L\omega_{0I}\{1/2Mn_M - 1/2(M+1)n_{M+1}\} \quad [13]$$

and the sum in Eq. [9] becomes just equal to $-S(N/2)$

$$\sum_{M=-N/2}^{N/2-1}\sum_{n=-\infty}^{\infty} S_n^M(0) = -Z^{-1}\beta_L\omega_{0I}N/2. \quad [14]$$

As a result the expected signal at $t = 0$ equals zero and $S(t)$ increases according to Eq. [9]. The actual time dependence of $S(t)$ must be evaluated by calculating the time-dependent matrix elements. This signal reaches a constant value when the interference between the oscillating terms in Eq. [9] reaches some average value. In systems with small values of *N* the CP signals of individual crystallites in a powder sample oscillate around an average value. However, the signal of a polycrystalline sample reaches some constant value that is equal to the sum of the signals of the individual single crystallites. The rise time of the CP signal can be calculated for a small spin system and is governed mainly by the interaction between the *S* spin and its nearest neighboring *I* spins. The *S* signal approaches its maximum value similarly to the decay of the FID signal of an *S* spin that is coupled to an ensemble of coupled *I* spins (*1*). In both cases the interference of the oscillating coherences contributing to the signal reaches an average value that is zero for the FID and different from zero for the CP signal. It is not a trivial task to calculate the CP *S*-signal intensity for long contact times. However, we can estimate the intensity of this CP signal by making some simple assumptions. Before doing so we must emphasize that in our discussion, all spin–spin and spin–lattice relaxation mechanisms are ignored.

CWCPMAS SIGNAL ENHANCEMENT

The average CP S signal can be estimated by using the following arguments. The CP process does not change the total energy of the spin system and does not change the eigenvalues of its density operator. At $t = 0$ the nonzero diagonal elements of the density matrix are determined by Eq. [7]. The values of these elements are the eigenvalues of the density matrix. For increasing CP mixing times the unitary evolution operator generates elements at different positions in the density matrix and changes the values $\langle M_p\alpha n|R(t)|M_p\alpha n\rangle$ and $\langle (M+1)_p\beta n|R(t)|(M+1)_p\beta n\rangle$ of the diagonal elements. For increasing N values the number of oscillating terms comprising these elements becomes large and it becomes useful to consider their time-averaged values. The time dependence of the off-diagonal and diagonal elements of $R(t)$ does not change its eigenvalues. However, the averaged off-diagonal elements become zero and the averaged diagonal elements reach a value that is not necessarily equal to these eigenvalues. Similar arguments are found in Sørensen's derivation of the universal bounds of polarization transfer experiments (*15*). We can estimate an upper bound for the CP S signal when we assume that the average values of all diagonal elements in each interacting manifold $\{|M\alpha n\rangle, |M+1\beta_m\rangle\}$ become equal.

The CP evolution of the spin system at the Hartmann–Hahn condition $\omega_{1I} - \omega_{1S} = k\omega_R$ can be described by following $R(t)$ in the $\{|M\alpha n\rangle, |M+1\beta n+k\rangle\}$ manifolds. Although the $\{|M_a\alpha n\rangle\}$ and $\{|M_a\beta n\rangle\}$ states are not the eigenstates of the total spin system, the diagonal elements of $R(t)$ in the representation of these states are called populations and their average values are defined by the population parameters

$$P(M_p,\alpha) = \overline{\langle M_p\alpha n|R(t)|M_p\alpha n\rangle}$$
$$P((M+1)_q,\beta) = \overline{\langle (M+1)_b\beta n+k|R(t)|(M+1)_b\beta n+k\rangle}, \quad [15]$$

where the bars represent time averaged values of the matrix elements. These parameters will reach some constant values in a time that is of the order of the inverse of the heteronuclear interaction strength. We estimate that the final values of the populations are equal to the average of the populations of the coupled levels at $t = 0$. At the Hartmann–Hahn condition these levels have nearly equal energy and this assumption does not violate the conservation of energy:

$$P(M_p,\alpha) = P((M+1)_q,\beta) = Z^{-1}\beta_L\omega_{0I}\frac{n_M M + n_{M+1}(M+1)}{n_M + n_{M+1}}. \quad [16]$$

Insertion of these parameters in the expression for the signal in Eq. [12] results in an upper bound for the normalized CPMAS signal:

$$S_{ub} = \frac{\omega_{0I}}{\omega_{0S}}\left\{\frac{1}{2}\sum_{M=-N/2}^{N/2} n_M\right\}^{-1} \times \left\{N/2 + \frac{1}{2}\sum_{M=-N/2}^{N/2-1}\frac{n_M - n_{M+1}}{n_M + n_{M+1}} \times (n_M M + n_{M+1}(M+1))\right\} = \frac{\omega_{0I}}{\omega_{0S}}\left\{\sum_{M=-N/2}^{N/2} n_M\right\}^{-1}\left\{\sum_{M=-N/2}^{N/2-1}\frac{2n_M n_{M+1}}{n_M + n_{M+1}}\right\}. \quad [17]$$

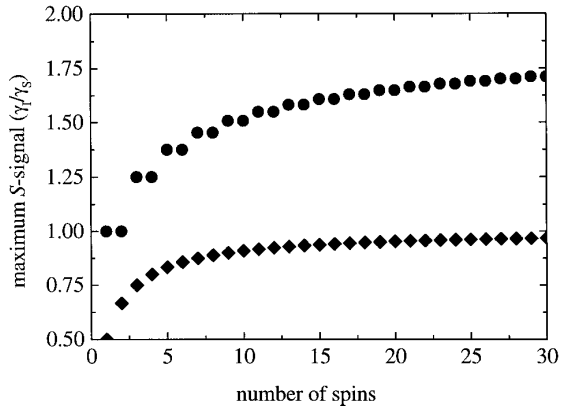

FIG. 2. The upper bounds of the relative CPMAS S-spin signal of a CWCPMAS (squares, according to Eq. [17]) and a fully adiabatic VACPMAS (circles, according to Eq. [20]) experiment as function of the number, N, of I spins in an $S(\frac{1}{2})I_N$ spin system.

This bound is plotted in Fig. 2 and represents the maximum signal that one can expect from a spin system with N I spins. For very large N its value approaches the spin-thermodynamic equilibrium value ω_{0I}/ω_{0S}, which is equal to the ratio between the magnetogyric ratios of the I and the S spins. The actual quasi-equilibrium state of the spin system at the end of a CP process will be characterized by a signal that is generally significantly smaller than S_{ub} and that depends on the geometry of the spin system and the NMR parameters. In static cross-polarization and spin diffusion experiments similar differences between quasi-equilibrium and ideal thermal-equilibrium states were studied experimentally and numerically (*12, 16–19*).

CWCPMAS SIGNAL SIMULATIONS

The simulations of the CPMAS S signals are performed for a model spin system of the form

$$CD_2H^a—{}^yCH_2^b—CH^c{=}CH^d—{}^xCOOH^e,$$

with a conformation of a d_2-pent-2-ene-oic acid molecule. CPMAS signals for singly ^{13}C-labeled molecules, with $x = 13$ and $y = 12$ or $x = 12$ and $y = 13$, are simulated as a function of the mixing time. In this publication the simulations are not yet compared with actual experimental results. However, the results provide a means for investigating thoroughly the CP spin dynamics and for ascertaining our ability to calculate CP signal enhancements in real experiments.

In order to obtain the magnitude of the S-spin signal as a function of the mixing time we used the expression (*5*)

$$S(t) = \{S(N/2)/S_0 + \sum_{M=-N/2}^{N/2-1} \sum_{r,s=1}^{n_M+n_{M+1}} \sum_{n} A_n^{rs}(M) \times \exp\{i(\lambda_n^r(M) - \lambda_0^s(M))t\}\} \quad [18]$$

with

$$A_n^{rs}(M) = S_0^{-1} \sum_k \{\langle\lambda_0^s|R_M(0) + R_{M+1}(0)|\lambda_k^r\rangle\}\langle\lambda_n^r|Z_S|\lambda_0^s\rangle. \quad [19]$$

The coefficients $A_n^{rs}(M)$ and frequencies $\lambda_n^r(M) - \lambda_0^s(M)$ are obtained from the diagonalization of the $\{|M\alpha n\rangle, |(M+1)\beta m\rangle\}$ Floquet matrix blocks and $S(N/2)$ from Eq. [10]. The normalization factor is proportional to the total number of I-spin levels in the system, according to Eq. [11]. Fourier analysis of Eq. [18] results in a frequency spectrum that can be constructed by adding signal intensities of magnitude $A_n^{rs}(M)$ at frequencies $\lambda_n^r(M) - \lambda_0^s(M)$. This CP spectrum, which is a function of the structure of the spin system, gives upon powder integration lineshapes that could be analyzed in terms of molecular structure in the same way as Fourier-transformed dipolar free induction decay signals.

In the actual calculations we evaluated the CPMAS S-spin signals in the frequency domain for a set of orientations of our model compound. CWCPMAS powder spectra were constructed by evaluation of the amplitudes $A_n^{rs}(M)$ at frequencies $\{\lambda_n^r(M) - \lambda_0^s(M)\}$ and the addition of the intensity $S(N/2)/S_0$ at zero frequency, as shown in Fig. 3. The lineshapes of these spectra can be compared with Fourier transforms of experimental CPMAS S-signal intensities as a function of the mixing time t, when they are independent of $T_{1\rho}$ rotating frame relaxation times. These shapes can be analyzed in terms of the molecular structure of the spin systems. The frequency axes of these spectra do not correspond to the rf irradiation frequencies or the frequencies of the free induction decay signals after cross polarization. Inverse Fourier transform of the simulated CPMAS spectra gives rise to the time-dependent signals shown in Fig. 4. For these calculations we assumed a spinning frequency of $\nu_R = 20$ kHz and conditions for the rf field intensities $\nu_{1I} - \nu_{1S} = 0$, 10, and 20 kHz. These three values correspond to the less-efficient H–H condition, $\Delta n = 0$, an intermediate case, and the efficient H–H condition, $\Delta n = 1$, respectively (*1*). The powder signals reach maximum values

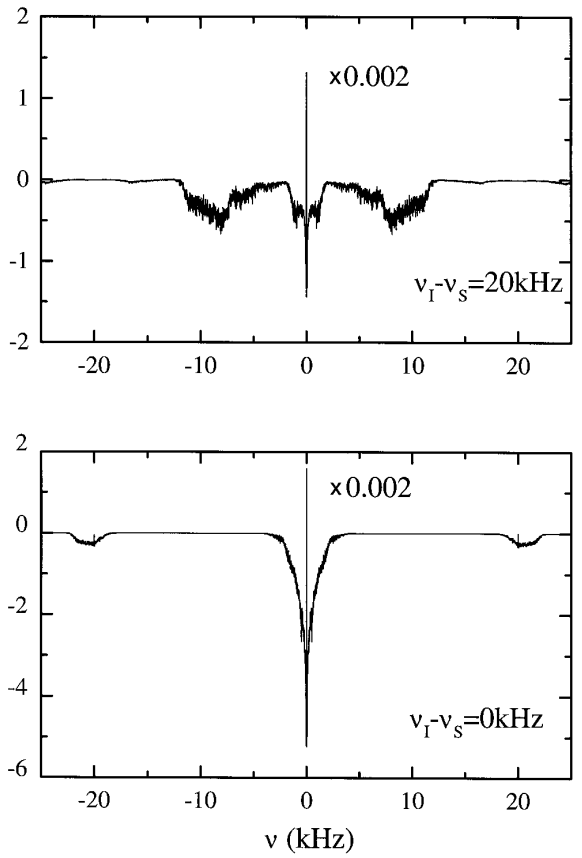

FIG. 3. The ^{13}C CWCPMAS frequency spectra of $^{13}CH_2$ in our six-proton model molecule for a spinning speed of 20 kHz and an rf amplitude difference ($\nu_{1I} - \nu_{1S}$) equal to 20 kHz at the $\Delta n = 1$ (top) Hartmann–Hahn condition and equal to 0 kHz at the $\Delta n = 0$ (bottom) Hartmann–Hahn condition. The integrated intensity of these spectra are zero and the center peak is generated mainly by the $S(N/2)$ signal contribution in Eq. [9]. Inverse Fourier transformation results in the S-spin CWCPMAS curves shown in Fig. 4.

that are smaller than the upper bound value of $0.86\gamma_I/\gamma_S$ for $N = 6$. As expected, the results for ^{13}COOH exhibit a much slower rise time than for $^{13}CH_2$. The time dependence of the S signal for $\nu_{1I} - \nu_{1S} = 40$ kHz, i.e., $\Delta n = 2$, is very similar to the results for $\Delta n = 1$.

For a spinning speed of 20 kHz the relative signal intensities at the $\Delta n = 1$, 2 H–H conditions reach a value that is of the order of $0.6\gamma_I/\gamma_S$. Similar values are obtained when we evaluate the signals for spin systems with only three interacting protons or when we ignore all homonuclear interaction terms in the Hamiltonian, even for the six-proton case (see Fig. 5). We must therefore conclude that at a spinning speed of 20 kHz the effective homonuclear dipolar interaction is so much reduced that it hardly influences the CP spin dynamics. In a recent publication (*20*) on calculations of MAS spectra of a six-proton spin system we showed that for $\nu_R = 20$ kHz the dipolar interaction is indeed significantly reduced. Thus it should be expected that the CP signal is almost solely determined by the heteronuclear dipolar interaction.

For the H–H condition with $\Delta n = 0$ the situation is more

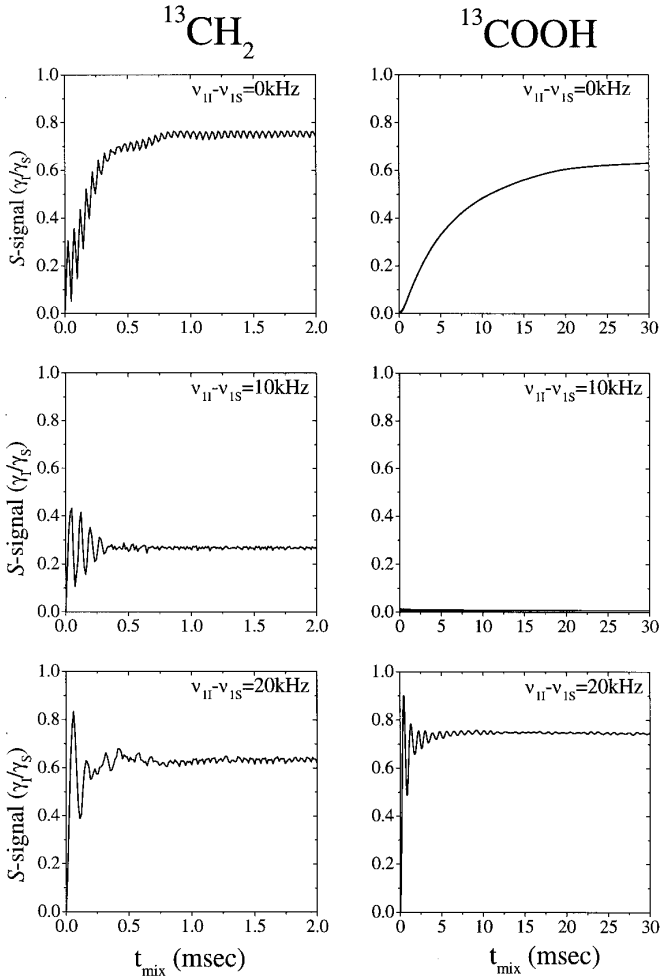

FIG. 4. Calculated ^{13}C CWCPMAS curves for the $^{13}COOH$ and $^{13}CH_2$ carbons of the $D_2HC—CH_2—CH═CH—COOH$ molecule at the Hartmann–Hahn conditions $\nu_{1I} - \nu_{1S} = 0$ kHz (top) and $\nu_{1I} - \nu_{1S} = 20$ kHz (bottom) for a spinning speed of 20 kHz. The results at the intermediate case, when $\nu_{1I} - \nu_{1S} = 1/2\nu_R$, is shown in the middle of the figure. These results demonstrate the difference between the CP efficiency of the direct and higher order Floquet state population equilibration at the $\Delta n = 1$ and $\Delta n = 0$ conditions, respectively. At a spinning speed of 20 kHz the homonuclear interaction is reduced significantly and for $\Delta n = 1$ the CP signal enhancement is governed mainly by the heteronuclear interaction. The CP process at $\Delta n = 0$ is possible only when there is a homonuclear interaction present and the effective reduction of this interaction slows down this process.

complicated. In this case the CP signal enhancement process is governed by an indirect process, where levels in the manifolds $\{|M\alpha n\rangle\}$ and $\{|M + 1\beta n\rangle\}$ are coupled via states $\{|M + 1\beta n + l\rangle\}$ and $\{|M\alpha n + l'\rangle\}$, with $l, l' = 2, 1, -1, -2$ (*5*). The S signal in the presence of the homonuclear interaction reaches its maximum value at a slow rate and exceeds the signals for $\Delta n = 1, 2$. For the $^{13}CH_2$ carbon the S signal reaches a value of $\sim 0.75\gamma_I/\gamma_S$, significantly higher than the value for $\Delta n = 1, 2$.

Some of the calculated signals show rotor-synchronized oscillations. Calculations of the CP signal enhancements for a spinning speed of 10 kHz gave results similar to those in Fig. 4 for $\Delta n =$ 0 and 1, and larger signals for the intermediate case $\nu_{1I} - \nu_{1S} =$ 5 kHz. The amplitudes of the oscillations were somewhat larger for $\nu_R = 10$ kHz than for $\nu_R = 20$ kHz.

Thus we can conclude that for high spinning speeds the CWCPMAS experiments on $^{13}C–^1H_N$ spin systems at the $\Delta n = \pm 1, \pm 2$ H–H conditions result in maximum carbon signals that do not increase for an increasing number, N, of protons. Only when the effective homonuclear interaction is significant can one expect a sufficient population redistribution that causes the signal to approach its upper bound value.

RAMPED VACPMAS SIGNALS

To simulate the S-spin signal as a function of the mixing time in a VACPMAS experiment the time-dependent spin evolution operator $U(0, t_{mix})$ of the $S(\frac{1}{2})I_N$ spin system must be evaluated. In our calculations we use the Floquet approach to evaluate this evolution operator. A variable amplitude of one of the rf fields results in a spin Hamiltonian that is not necessarily periodic in time. In our calculations we considered an rf field difference $\Delta\omega(t) = \omega_{1I}(t) - \omega_{1S}(t)$ that was increased synchronously with the sample spinning. The amplitudes of the fields were kept constant during each rotor period and were modified only at times $t = \kappa k T_R$, with $T_R = 2\pi/\omega_R$ and $\kappa = 0, 1, 2 \ldots$. The Floquet Hamiltonian H_F^κ during each time interval, $\kappa k T_R \rightarrow (\kappa + 1)kT_R$, was constructed for a constant $\Delta\omega(\kappa)$ value and the matrix elements of $U(\kappa k T_R, (\kappa + 1)kT_R)$ were derived from the elements of the Floquet evolution operator (*1, 5*). The time-independent Floquet matrix during each time interval was again subdivided into diagonal blocks, defined by the manifolds $\{|M\alpha n\rangle, |(M + 1)\beta m\rangle\}$, and diago-

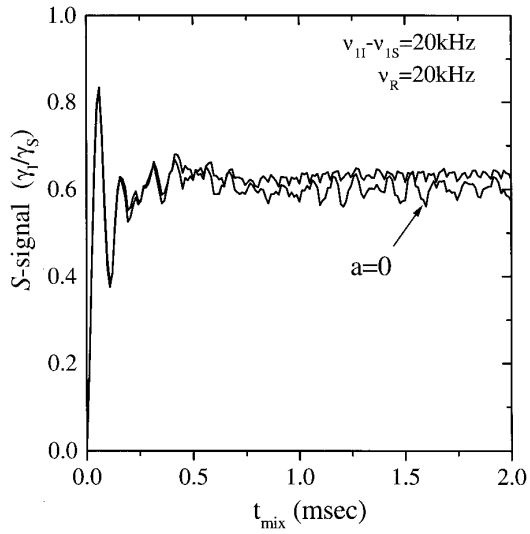

FIG. 5. A comparison between the ^{13}C CWCPMAS curve of the $^{13}CH_2$ carbon in our model compound at the $\Delta n = 1$ Hartmann–Hahn condition and the curve calculated for the same carbon assuming a zero homonuclear interaction ($a = 0$) between the protons. This result is an indication of the effective reduction of the homonuclear interaction at a spinning speed of 20 kHz.

nalized sequentially. The elements of the spin evolution operator, such as (*4, 5*)

$$\langle M_p\alpha|U(\kappa kT_R,\ (\kappa+1)kT_R)|M_q\alpha\rangle = \sum_n \langle M_p\alpha n|\exp\{-iH_F(t_m)\times kT_R\}|M_q\alpha 0\rangle,$$

were then calculated and the signal was obtained by the matrix multiplication

$$U(0,\ KT_R) = \prod_{\kappa=0}^{K-1} U(\kappa kT_R,\ (\kappa+1)kT_R)$$

and

$$S(KT_R) = \frac{\omega_{0I}}{\omega_{0S}}\{\sum_{M=-N/2}^{N/2} n_M\}^{-1} \times\{N + \sum_{M=-N/2}^{N/2-1}\sum_{p=1}^{n_M} M|\langle M_p\alpha|U(0,\ KT_R)|M_p\alpha\rangle|^2 - \sum_{M=-N/2+1}^{N/2}\sum_{p=1}^{n_M} M|\langle M_p\beta|U(0,\ KT_R)|M_p\beta\rangle|^2\}. \quad [20]$$

In Fig. 6 the ramped VACPMAS signals as a function of the mixing time are shown for the ^{13}COOH and $^{13}CH_2$ carbons in our six-proton model system. In these calculations the rf field differences were increased, as shown in the figure, and the sample spinning frequency was 20 kHz. Starting at values of −10 and 10 kHz the difference was increased in 60 steps up to values of 10 and 30 kHz, respectively. During the mixing time the spin system passes, respectively, through the $\Delta n = 0$ and 1 H–H condition, causing a level crossing of the manifold of Floquet states $|M_p\alpha n\rangle$ and $|(M+1)_q\beta m\rangle$. This ramped amplitude CPMAS experiment can cause population exchange between coupled states, when their level crossing is adiabatic (*1, 7, 20*). These population redistributions will again result in an *S*-spin signal enhancement.

Just as for the CWCPMAS experiment the above results can be compared with the maximum possible signal that can be expected in these experiments. The upper bound for different *N* values can be estimated when we assume that the level crossings are pairwise and adiabatic (*15, 21*). With these assumptions the n_M states of $\{|M\alpha n\rangle\}$ and n_{M+1} states of $|(M+1)\beta n+1\rangle$, for each *n* and for example $\Delta n=1$, interchange their populations a number of times, which is equal to the smallest of the two values n_M and n_{M+1}. After a full adiabatic passage the diagonal elements of the final Floquet density matrix are equal to the diagonal elements of the initial density matrix. This rearrangement of elements does not change the eigenvalues of the density matrix and the populations in Eq.

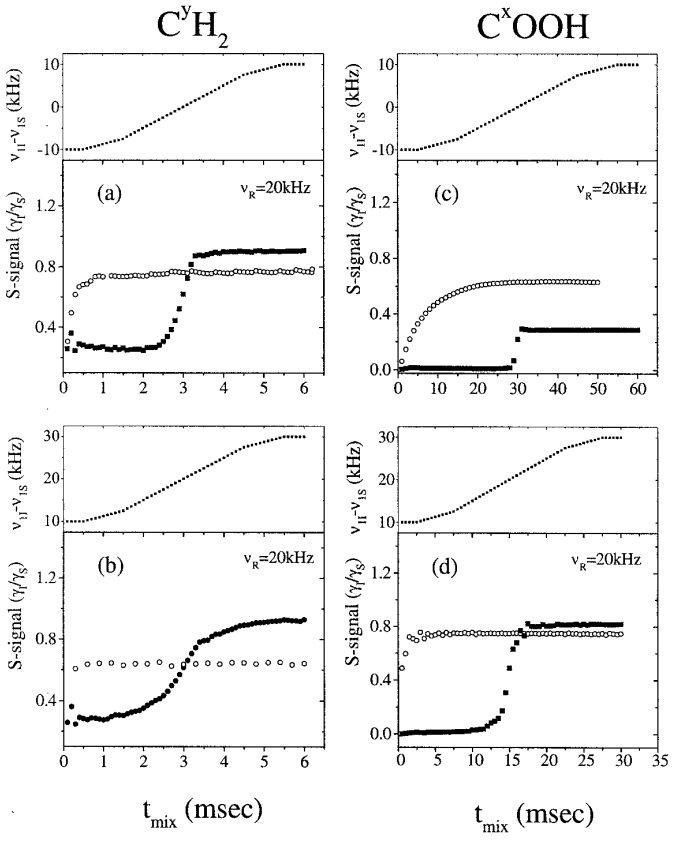

FIG. 6. The ^{13}C VACPMAS signal enhancement (filled circles) of the ^{13}COOH and the $^{13}CH_2$ carbons in our model compound. The time dependences of ($\nu_{1I}-\nu_{1S}$) in these ramped amplitude CPMAS experiments are shown for the four calculations. These rf intensity differences are passing through the $\Delta n = 0$ and 1 Hartmann–Hahn conditions. These CP results are compared with the CWCPMAS results (open circles) at the exact $\Delta n = 0$ and 1 conditions. The maximum ^{13}C signals are significantly smaller than the upper bound signal for $N = 6$ in Fig. 2.

[15] do not need any time averaging. A straightforward calculation results then in the normalized upper bound signal for the adiabatic ramped amplitude CPMAS experiment for an even number *N* of *I* spins of the form

$$S_{ub} = \frac{\omega_{0I}}{\omega_{0S}}\sum_{M=N/2}^{0}(n_M - n_{M+1})M + n_{M+1} \quad [21]$$

with $n_M = 0$ for $M > N/2$. In Fig. 2 this bound is shown as a function of the number of *I* spins in the $S(\frac{1}{2})I_N$ system. For example, for $N = 100$ the value S_{ub} equals $1.84\gamma_I/\gamma_S$. As can be seen in Fig. 6 the signals of the six-proton system do not reach their upper bound, which is equal to 1.37 for $N = 6$. This is an indication that the level-crossing process is more complicated than according to the adiabatic assumption. This should not surprise us, when we consider the number of states that are undergoing the quasi-adiabatic process simultaneously, even in our relatively simple model molecule.

To demonstrate the complexity of the process we show in

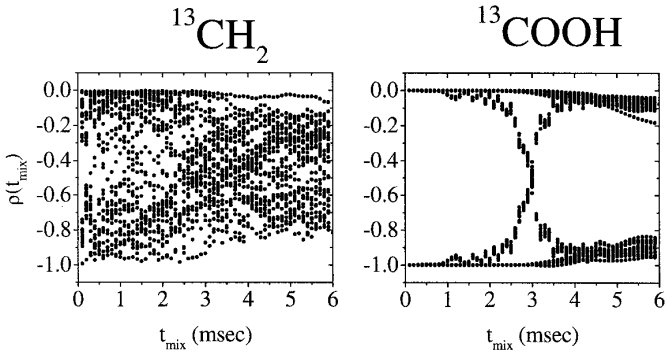

FIG. 7. The time dependence of the diagonal elements $P_i(t_{\mathrm{mix}})$ equal to $\langle M_p\alpha|\rho(t_{\mathrm{mix}})|M_p\alpha\rangle$ and $\langle(M+1)_q\alpha|\rho(t_{\mathrm{mix}})|(M+1)_q\beta\rangle$ of the ^{13}COOH and $^{13}CH_2$ carbon spin density matrix, $\{\rho(t_{\mathrm{mix}})\}$, for $M=-1$, $p=1,\ldots,15$, $q=1,\ldots,20$, and $i=1,\ldots,35$, of a single crystallite of our model compound. These elements are calculated for the ramped amplitude CPMAS experiment shown in Figs. 6b and 6d, with a spinning speed of 20 kHz. For ^{13}COOH the process is almost adiabatic, because the diagonal elements at the end of the mixing time are about equal to their initial values at $t_{\mathrm{mix}}=0$. For the $^{13}CH_2$ carbon the CP process is far from adiabatic as can be seen from the variations in the 35 diagonal matrix elements during the contact time.

Fig. 7 the time dependence of the 35 diagonal elements of the spin density matrix belonging to the $\{|(M=-1)\alpha\rangle; |(M=0)\beta\rangle\}$ subspace of a single crystallite of our model molecule. These elements were calculated for the experiment presented in Figs. 6b and 6d. At $t=0$ these values are equal to the initial populations -1 and 0 of the $|(M=-1)\alpha\rangle$ and $|(M=0)\beta\rangle$ spin states, respectively. If the CP process is purely adiabatic these values should again be equal to -1 and 0 at the end of the mixing time. That this is not so can be learned from the results of $^{13}CH_2$ and ^{13}COOH shown in Fig. 7.

Modifications in the ramped amplitude of the VACPMAS experiment will result in different final populations and an optimization of the shape of $\Delta\omega(kT_{\mathrm{R}})$ could result in some maximum powder signal. This was not done here, and discussions about optimization of the shapes of the rf fields can be found in the literature (*7*, *8*).

SUMMARY AND DISCUSSION

In this publication we have demonstrated the use of Floquet formalism to calculate CPMAS signals. The size of the spin system that can be treated with this approach is restricted by the time it takes to diagonalize large matrices. For example, the calculations of a whole CPMAS powder spectrum, as in Fig. 3, takes 6 h of CPU time and a VACPMAS curve, as in Fig. 6a, takes 24 h of CPU time for 300 crystallite orientations on an ALPHA DEC station, without using parallel computing. The emphasis of our discussion was on the methodology of computation. At a later stage these calculations will be used to analyze experimental CWCPMAS results and to optimize VACPMAS methods in particular for high field experiments on samples spinning at frequencies larger than 20 kHz. Then the CP process can become independent of the homonuclear interaction and the *S*-signal enhancement can be evaluated by multiplying the cosine functions, describing the time dependence of the signal on the heteronuclear interactions between the *S* spin and the individual *I* spins. In addition the influence of spin–lattice relaxation and molecular motion on the CPMAS curves should be considered in the future. This would require an extension of our program by taking dynamic NMR Floquet theory into account.

For large spin systems it will be necessary to use approximate methods to evaluate the influence of *I* spins that are not directly coupled to the *S* spin. In the CWCPMAS calculations this can be achieved by a line broadening of the CPMAS frequency spectrum and an increase of its center frequency value. In the case of the ramped VACPMAS experiments this is more difficult and more efficient computational methods must be developed.

ACKNOWLEDGMENTS

We thank Dr. Madhu for stimulating discussions. This work was supported by the Israeli Science Foundation.

REFERENCES

1. D. Marks and S. Vega, *J. Magn. Reson. A* **118,** 157 (1996).
2. A. Pines, M. G. Gibby, and J. S. Waugh, *J. Chem. Phys.* **59,** 569 (1973).
3. E. O. Stejskal, J. Schaefer, and J. S. Waugh, *J. Magn. Reson.* **28,** 105 (1977).
4. A. Shmidt and S. Vega, *J. Chem. Phys.* **96,** 2655 (1992).
5. O. Weintraub and S. Vega, *J. Magn. Reson. A* **105,** 245 (1993).
6. O. Peersen, X. Wu, I. Kustanovich, and S. E. Smith, *J. Magn. Reson. A* **104,** 334 (1993).
7. S. Hediger, B. Meier, and R. R. Ernst, *Chem. Phys. Lett.* **213,** 627 (1993).
8. S. R. Hartmann and E. L. Hahn, *Phys. Rev.* **128,** 2042 (1962).
9. S. Zhang, C. L. Czekaz, and W. T. Ford, *J. Magn. Reson. A* **111,** 87 (1994).
10. D. A. McArthur, E. L. Hahn, and R. E. Walstedt, *Phys. Rev.* **188,** 609 (1969).
11. D. Demco, J. Tegenfeldt, and J. S. Waugh, *Phys. Rev. B* **11,** 4133 (1975).
12. M. H. Levitt, D. Suter, and R. R. Ernst, *J. Chem. Phys.* **84,** 4243 (1986).
13. M. Maricq and J. S. Waugh, *J. Chem. Phys.* **70,** 3300 (1979).
14. A. E. Benett, R. G. Griffin, and S. Vega, *in* "NMR Basic Principles and Progress," Vol. 33, p. 1, Springer-Verlag, Berlin/Heidelberg (1994).
15. O. W. Sørensen, *J. Magn. Reson.* **86,** 435 (1990); **93,** 648 (1991).
16. P. M. Hendrichs and M. Linder, *J. Magn. Reson.* **58,** 458 (1984).
17. P. Robyr, B. H. Meier, and R. R. Ernst, *Chem. Phys. Lett.* **187,** 471 (1991).
18. R. Bruschweiler and R. R. Ernst, *Chem. Phys. Lett.* **264,** 393 (1997).
19. D. K. Sodickson and J. S. Waugh, *Phys. Rev. B* **52,** 6467 (1995).
20. S. Ray, G. J. Boender, E. Vinogradov, and S. Vega, *J. Magn. Reson.* **135,** 418 (1998).
21. A. Abragam, "Principles of Nuclear Magnetism," Academic Press, New York (1962).